Check for updates

Quinazolin derivatives as emerging alpha-glucosidase inhibitors

Ashok Reddy Ankireddy [iD] 1, Rambabu Gundla [iD] 1,*, Tuniki Balaraju [iD] 2, Venkanna Banothu [iD] 3, Krishna Prasad Gundla [iD] 1, Uma Addepally [iD] 3 and Jithendra Chimakurthy [iD] 4

1 Department of Chemistry, Gitam University, Hyderabad, Rudraram Mandal, Sangareddy District, Patancheru, Hyderabad, Telangana 502329, India
ankireddyashokreddy@gmail.com (A.R.A.), rambabu.gundla@gitam.edu (G.R.), krishnaprasadgundla@gmail.com (K.P.G.)
2 Department of Chemistry, Birla Institute of Technology, Mesra, Jharkhand 835215, India
balarajutuniki@gmail.com (T.B.)
3 Centre for Biotechnology (CBT), Institute of Science & Technology (IST), Jawaharlal Nehru Technological University Hyderabad (JNTUH), Kukatpally, Hyderabad, Telangana State, 500085, India
venky.bt@gmail.com (V.B.), vedavathi1@gmail.com (U.A.)
4 Department of Pharmaceutical Sciences, Vignan's Foundation for Science, Technology and Research Vadlamudi, Guntur, Andhra Pradesh 522213, India
jithendrach@gmail.com (J.C.)

* Corresponding author at: Department of Chemistry, Gitam University, Hyderabad, Rudraram Mandal, Sangareddy District, Patancheru, Hyderabad, Telangana 502329, India.
Tel: +91.863.2344700 Fax: +91.863.2344700 e-mail: rambabu.gundla@gitam.edu (G. Rambabu).

RESEARCH ARTICLE

ABSTRACT

A series of C-7 substituted-2-morpholino-*N*-(pyridin-2-ylmethyl)quinazolin-4-amine have been synthesized and biochemical assay was examined against α-glucosidase function inhibition activity. A structure activity and structure property relationship study was experimented to surface the new hit compound. This study led to the identification of C-7substituted quinazolines with minimum inhibitory concentrations (MICs) in the preffered micromolar range in addition with interesting physicochemical properties. Biological evaluation yielded eight analogs which rose with significant α-glucosidase inhibition potency (IC$_{50}$ values < 2 μM, where reference compound (Acarbose) potency value is IC$_{50}$ = 0.586 uM) and could be promising candidates for further lead optimization.

Cite this: *Eur. J. Chem.* **2018**, *9(4)*, 322-330 | **Journal website**: www.eurjchem.com

1. Introduction

The complex and acute health condition of the current generation which rise from irregular or excess food consumption, lack of regular exercise (physical) or rarely genetically that is diabetes mellitus delineate the critical metabolic disorder of multiple etiologies characterized by chronic hyperglycemia with disturbances of carbohydrate, fat and protein metabolism, consequences defects in insulin secretion, action and frequently both. According to a recent pandect approximately 366 million people are suffering from this health disorder across the globe and this number is estimated to increase 522 million by 2030 [1]. It is also a common endocrine disorder characterized by hyperglycemia, which has become a major risk to the individual's quality of life. The effects of diabetes mellitus include long-term damage, dysfunction and failure of various organs. It may present with characteristic symptoms such as thirst, polyuria, blurring of vision, and weight loss, in its most severe forms ketoacidosis or a non-ketotic hyperosmolar state may raise and lead to apathy, coma and in absence of effective treatment leads to death [2]. With subject to control this particular disease, one of the best-studied therapeutic target is α-glucosidase and its function inhibition. It is located in the brush border of the small intestine [3-7] and involved in breaking down complex carbohydrates such as starch and glycogen into their monomers, it catalyzes the cleavage of individual glucosyl residues from various glycoconjugates including alpha or beta linked polymers of glucose. The body system which is affected by diabetes mellitus needs external regulators to control the insulin balance in the blood, here the α-glucosidase inhibitors come into action, α-glucosidase inhibitors decrease both postprandial hyperglycemia and hyperinsulinemia, and thereby may improve sensitivity to insulin and release the stress on beta cells [7].
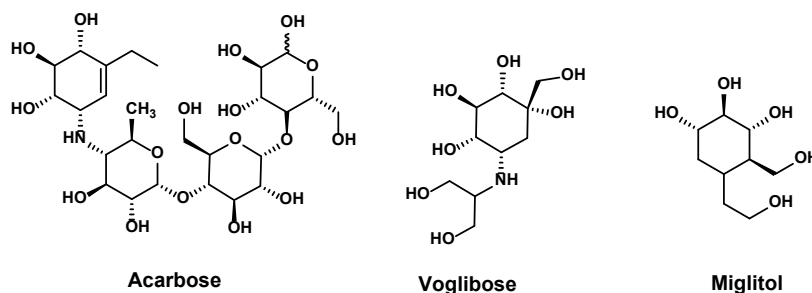
Figure 1. Chemical structure of sugar mimics α-glucosidase inhibitors.

One of the strategies for the management of diabetes is appropriate drug administration to control postprandial hyperglycemia [8,9]. Many α-glucosidase inhibitors have also been observed as potential anti-cancer agents, antiviral infections, and anti-proliferation in Human Immunodeficiency Virus (HIV) infections, making the compounds with multiple therapeutic targets. α-glucosidase inhibitors also have considerable potential for preventing these cardiovascular risks [10].

Till date, although significant progress has been made to invent new class of α-glucosidase inhibitors for the treatment of diabetes [11-15] most of the developed ones are sugar mimics (Figure 1) which require tedious chemical procedures [16], low yield, long reaction conditions and high temperature reactions. At present, a large number of compounds mimicking the structures of monosaccharides or oligosaccharides have been discovered from natural sources, which include thio-sugars [17-19], nitrogen containing α-glucosidase inhibitors [20]. Among the multifarious biologically active heterocyclic compounds, nitrogen containing heterocycles play a vital role in controlling postprandial glucose [21]. In fact, recent surveys have reported that a high number of molecules currently under scrutiny by researchers, which contain nitrogen containing heterocyclic chemical compounds, from those, quinazoline and quinazolinone derivatives are found at most important family of compounds [22-24]. The synthesized compounds (quinazolines) have a common unique structural framework, which we were able to use for the scaffold diversification, which is useful for the preparation of pharmacological entities [25]. So far, in the literature, research on quinazolin-4(3*H*)-ones have been carried out on the C-2, N-3, C-4 and C-6 positions of the core structure [26]. A very few literature evidences have been studied on the extension of C-7 position of the core structure [20,27,28]. Therefore, there is a substantial enthusiasm in developing efficient methods for the synthesis of C-7substituted-2-morpholino-*N*-(pyridin-2-ylmethyl)quinazolin-4-amine. Recently, we published few proficient palladium catalysed synthetic method for the introduction of substituted amino groups at the C-6 position of 2-cyclopropyl-3-(pyridyl-3ylmethyl)quinazolin-4(3*H*)-one with impressive yields. These scaffolds further modified at C-4 position using amidation [23]. Here in this article, we report a lead α-glucosidase inhibitor from a series of 20 novel quinazoline derivatives. The binding mode of the compounds and all molecules (SAR) including reference compound acarbose at the active site of alpha-glucosidase was explored using Glide [26] also here we report drug-like properties of the all chemical entities by in-silico experiments.

2. Experimental

2.1. Synthesis

For the present work, 7-chloro-2-morpholino-*N*-(pyridin-2-ylmethyl)quinazolin-4-amine synthesized intermediate **7**

was chosen as a key starting material for the study, and the first two steps were conveniently synthesized by known procedures [2]. The compound 2,4,7-trichloroquinazoline (Compound **3**) was synthesized by cyclisation with 2-amino-4-chlorobenzoic acid with urea at neat, 200 °C, 8 h, the reaction mixture was diluted with water, filtered and dried to give 7-chloroquinazoline-2,4(1*H*,3*H*)-dione (Compound **2**).

The obtained compound **2** was chlorinated with POCl₃, *N*,*N*-dimethylaniline, reflux for 8 h, and then allowed to cool to room temperature and poured in to ice cold water. The resulting solid was collected by filtration and dried to give pure 2,4,7-trichloroquinazoline (Compound **3**). To the solution of 2,4,7-trichloroquinazoline (Compound **3**) in THF was added pyridin-2-ylmethanamine, stirred at room temperature for 12 h to give the 2,7-dichloro-*N*-(pyridin-2-ylmethyl)quinazolin-4-amine (Compound **5**), followed by the reaction with morpho-line in isopropyl alcohol, DIPEA stirred at 100 °C for 12 h. The crude compound was purified by combi flash chromatography to give pure 7-chloro-2-morpholino-*N*-(pyridin-2-ylmethyl) quinazolin-4-amine (Compound **7**) (Scheme 1). Compound **7** was modified at C-7 position by utilizing Suzuki-Miyaura cross-coupling reaction conditions to obtain novel substituted quinazolinones. Based on our previous experience on C–C cross-coupling reactions, we have chosen Pd(PPh₃)₄, PdCl₂ (PPh₃)₂, PdCl₂(dcpf), Pd(dppf) and Pd(OAc)₂ as different palladium-based pre-catalyst systems for screening with different bases like K₂CO₃, Na₂CO₃, Cs₂CO₃ and K₃PO₄ in solvents 1,4-dioxane:H₂0 (3:1, *v:v*), THF:H₂0 (3:1, *v:v*) and toluene:H₂O (3:1, *v:v*) at reflux. But, all of the methods failed to yield substituted quinazolinones.

The initial experiments were performed without using any ligand and were unsuccessful to prepare compounds **8** to **27**. The development of easy synthetic strategies for the const-ruction of carbon-carbon bonds with palladium catalyzed Suzuki-Miyaura cross-coupling reactions remains an impor-tant challenge in organic synthesis. 7-Chloro-2-morpholino-*N*-(pyridin-2-ylmethyl)quinazolin-4-amine were chosen for the present study. The overall aim was not only to determine the best conditions for Suzuki-Miyaura cross coupling reactions, but also to find the optimal conditions that can be applied for the synthesis of a broad range of 7-aryl, heteroaryl, and biphenyl quinazolin-4-amine. Optimization experiments were carried out using Pd(PPh₃)₄, PdCl₂(PPh₃)₂, PdCl₂(dcpf), PdCl₂(dtbpf), PdCl₂(dppf), Pd(OAc)₂ and Pd₂(dba)₃ as metal sources, ligands L1–L6 (Figure 2) were selected for combi-nation with the metal. After trying several combinations of catalyst and ligand in different bases K₂CO₃, Na₂CO₃, Cs₂CO₃ and K₃PO₄, we optimized the conditions in microwave Pd(OAc)₂, X-PHOS, K₃PO₄, THF, H₂O (3:1), 120 °C, 30 min, and prepared compounds **8** to **27** in 62 to 88% yield (Scheme 2). After finalizing the optimal conditions, several boronic acids were employed which underwent cross coupling reactions at 120 °C, 30 min, and microwave to produce the analogs shown in Table 1.
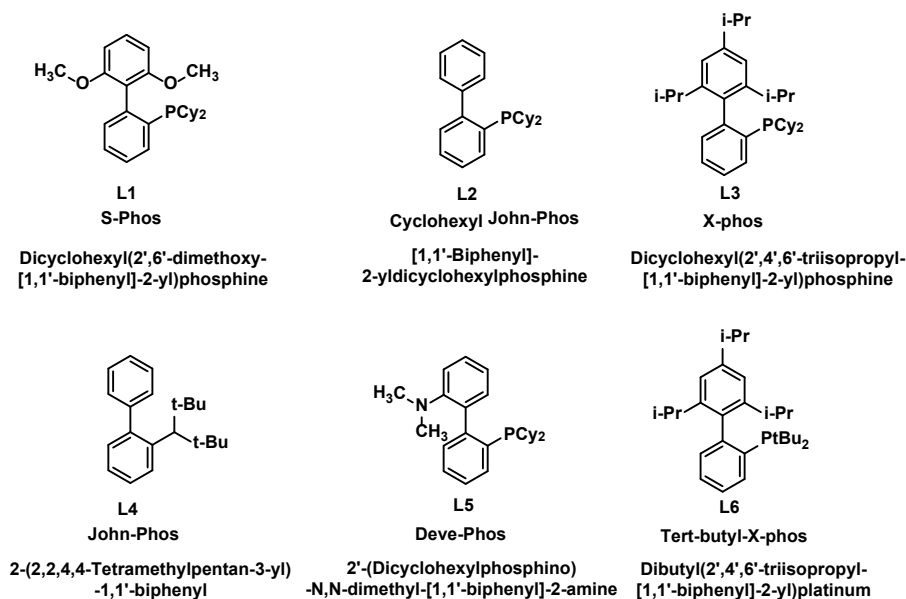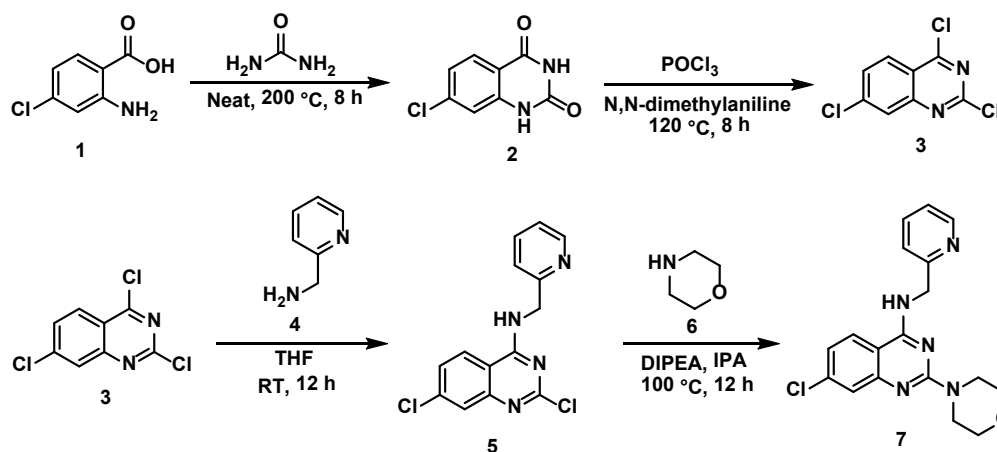
Figure 2. Structure of ligands used in Suzuki reactions.

Scheme 1. Synthesis of 7-chloro-2-morpholino-*N*-(pyridin-2-ylmethyl)quinazolin-4-amine (Compound 7).

From Table 1, it is clear that a wide assortment of aryl, heteroaryl and biphenyl boronic acids undergo Pd-catalyzed Suzuki-Miyaura cross coupling reactions. The final C–C coupling products of boronic acids with electron withdrawing groups like 2-carboxylicphenyl boronic acid (Entry 15, 88%), and least yield in electron donating group like 2-methoxy-phenyl boronic acid (Entry 4, 62%).

After attempting several reactions, we concluded that, after adding ligand in Suzuki coupling reaction on compound **7**, and then there is a formation of desired products **8** to **27**. Later, we screened different ligands with different catalyst, by changing bases and solvents. We concluded that Ligand L3 (X-Phos) on compound **7**, and K_3PO_4 as a base, this condition gives some desired product and also THF was superior to 1,4-dioxane and PhMe, the ratio of THF and H_2O is (4:1, *v:v*). From these data, $Pd(OAc)_2$/L3 (X-Phos) was superior to the other biaryl-ligand-based catalysts, which gave product yields in the range of 4–30% with a catalytic loading of metal of 5 or 10 mol%. The reaction of 10 mol% $Pd(OAc)_2$ in the presence of THF was superior compared to 1,4-dioxane 80 °C for 16 h. Whereas, when the reactions were conducted in the case of 5 mol% $Pd(OAc)_2$, THF yields didn't change appreciably, and also reactions were carried out with 10 or 20 mol% of catalyst
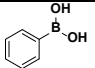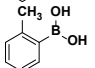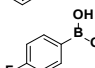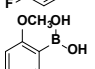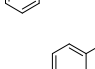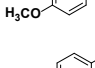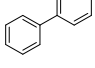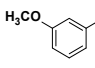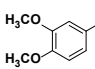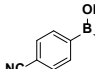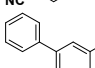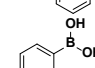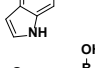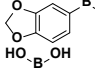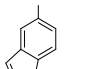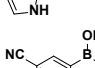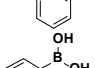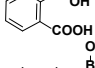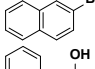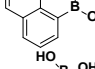
using also yields didn't change appreciably. After identifying 10 mol% $Pd(OAc)_2$ in combination with X-Phos, K_3PO_4, THF and H_2O is (4:1, *v:v*), we focused to increase the yield in the C–C cross coupling reactions. Then, we performed Suzuki coupling reactions in Microwave instruments, there we got better results. Results from our initial investigations [29] by using ligand are shown in Table 1.

2.2. Molecular modelling and drug design

Molecular Modeling and analysis: The binding mode of the compounds at the active site of a-glucosidase was explored using Glide In-silico protocol (Schrödinger software package Maestro 2017-2 (Glide, Schrödinger, LLC, New York, NY, 2017). A search of a 3D database (GOSTAR) we prioritized the synthesis molecules. The PDB ID 3WY1 was used for docking study which was downloaded from protein data bank (www.rcsb.org).

Ligand preparation: All ligands were drew by using maestro (Schrödinger Software) and prepared for docking by ligprep module (LigPrep, Schrödinger, LLC, New York, NY, 2017).

Table 1. Evaluation of the scope of C–C coupling reactions of various boronic acids with 7-chloro-2-morpholino-*N*-(pyridin-2-ylmethyl)quinazolin-4-amine by using ligand (L3) (Scheme 2) *.

Molecule Number	Boronic acid derivative	Yield (%)		
		K₃PO₄, THF:H₂O (4:1), Microwave, 120 °C, 30 min,	K₃PO₄, THF:H₂O (4:1), Sealed tube, 100 °C, 60 min	K₃PO₄, THF:H₂O (4:1), Conventional, 80 °C, 16 h
8		80	60	30
9		65	42	21
10		77	53	13
11		62	35	20
12		66	41	22
13		67	54	18
14		75	35	15
15		65	65	17
16		75	25	14
17		67	40	5
18		81	55	6
19		88	65	11
20		81	61	16
21		75	60	5
22		88	55	7
23		75	58	15
24		71	41	8
25		69	55	4
26		75	45	12
27		70	44	15

* All reactions were carried out in 10 mg scale initially. After succeeding the product formation in Pd(OAc)₂, X-PHOS, K₃PO₄, THF: H₂O (4:1, *v:v*), then we focused to increase the yields. Reactions were initially carried out in conventional method. The yields were gradually increased when we changed from conventional to sealed tube. Finally the yields were much better when we used microwave 120 °C, 30 min. best yields were observed for compound **19** and **22**.
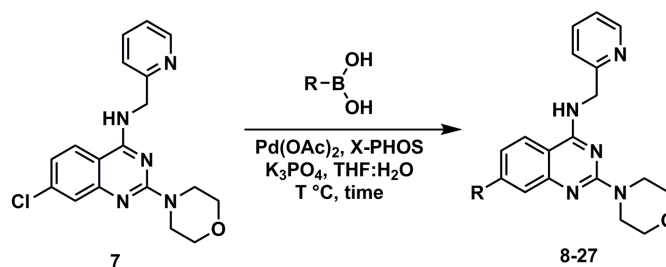
Scheme 2. Synthesis of 7-substituted quinazoline compounds.

The docking in-silico experiments were performed through Glide (Grid based Ligand Docking with Energetics) program in Schrödinger Software (Maestro) Suite. In Glide, the initial filters test the spatial fit of the ligand to the defined active site and examine the complementarity of ligand-receptor interactions using a grid-based method patterned after the empirical ChemScore function. Poses that pass these initial screens enter the final stage of the algorithm, which involves evaluation and minimization of a grid approximation to the OPLS-AA non-bonded ligand-receptor interaction energy. Final scoring was then carried out on the energy-minimized poses. By default, Schrödinger's proprietary GlideScore multi-ligand scoring function is used to score the poses. Emodel which is used to rank the poses, combines GlideScore, the non-bonded interaction energy and for rigid docking, the excess internal energy of the generated ligand conformation.

2.3. Preparation of protein structures

The crystal structure of tubulin (PDB id 3WY1) was considered to get insights into the binding modes of ligands. The protein X-ray structure was prepared using the Protein Preparation Wizard implemented in Maestro 11.4 (Schrödinger, LLC, New York, NY, 2017) with the following steps (i) the missing side chains were added to the crystal structure by Schrödinger's Prime 3.0. (ii) Hydrogen bond atoms were added and water molecules within 5 Å of the co-crystallized ligand were removed. (iii) Protonation states of entire systems were adjusted to the pH range of 7.0+/-4.0 using Epik. (iv) Hydrogen bond networks and flip orientations/tautomeric states of Gln, Asn, and His residues were optimized. (v) The geometry optimization was performed to a maximum root mean square deviation (RMSD) of 0.3 Å with the OPLS2005 force field.

2.4. Receptor grid generation and docking

Grid was generated using receptor grid generation in Glide program. The binding region was defined using a co-crystal ligand. Docking Studies Docking has performed with the solved 3D-structure of α-glucosidase (PDB id 3W37), using Glide module in Schrodinger. The authenticity of this docking method to predict the bioactive conformation was validated using the X-ray structure of acarbose in complex with a co-crystal acarbose. Co-crystal acarbose was redocked into the active site of 3WY1 and the best predicted bound conformation having lowest docking energy was selected. Glide uses an explicit water model for modelling salvation effects [30,31]. The demonstrated research output and results are the structural model exploration and involved methodology is very effective, which was analyzed in few of research papers also [21,25,32]. In this methodology, we taken G-score, which is a modified and extended empirical scoring function based on Chem-Score the docking method that is XP descriptors been used to score [33,34] (G-score) for ligand includes drug like

properties such as Lipo-EvdW, H-bond, and RotPenal. Lipo-EvdW is the Chem-Score lipophilic pair term and fraction of the total receptor-ligand VdW's energy. H-bond is the Chem-Score H-bonding pair term. Non-H-bonding polar/hydrophobic interactions following generation of hydrophobic-hydrophilic surfaces [21,32,35].

2.5. Biology assays

α-Glucosidase inhibitory assay: The inhibitory effect of the synthesized compounds on α-glucosidase inhibitory activity was determined in 96-well plates employing the substrate PNPG and 4-nitrophenyl α-D-glucopyranoside according to the procedure previously reported by Ferreres *et al.* [2]. Prior to use, all test compounds were solubilised in solvent, dimethylsulfoxide (DMSO). Briefly, each well in 96-well plates contained 100 μL of 2 mM 4-nitrophenyl α-D-glucopyranoside (PNP-G) in 10 mM potassium phosphate buffer (pH = 7.2) and different test concentrations (20-100 μg/mL). The reaction was initiated by the addition of 5 μL of the enzyme solution (0.1 IU per well), α-glucosidase (obtained from baker's yeast purchased from Sigma Aldrich, Bangaluru). The plates were incubated at 37 °C for 10 min. The absorbance was measured spectrophotometrically at 430 nm (Spectra Max M5e micro plate reader). The increase in absorbance (ΔA) was compared with that of the control (buffer instead of test compound) to compute the inhibitory concentrations (IC_{50}) which was determined from three independent assays. Acarbose, an illustrious inhibitor of α-glucosidase was employed as positive control.

$$Inhibition\ (\%) = (\Delta A_{control} - \Delta A_{sample}/\Delta A_{control}) \times 100 \qquad (1)$$

The concentration of compound required to obtain 50% inhibition of α-glucosidase activity under the assay conditions was defined as the IC_{50} value.

2.6. In-vitro studies

Grouping and preparation of animals: Rats were randomly divided into 8 groups each containing 10 animals; Control group, negative control group (STZ), A group, B group, C group, D group, E group, positive control group (PIO). Control group was fed with standard chow (calorific value, 20-22 kJ/kg) and all the other groups were fed with high fat diet obtained from Rayan's Biotech (calorific value, 43-45 kJ/kg) for 4 weeks. STZ 45 mg/kg (freshly prepared acetate buffer 0.1 M, pH = 4.5) was administered intraperitoneally to all the groups except control (buffer alone). After 8 weeks of STZ administration, rats were fasted for 12 hrs and the fasting blood glucose levels were measured using tail vein method, rats with fasting blood glucose levels above 250 mg/dL were considered to be diabetic and used for the study. Rats were allowed to feed on their respective diets until the end of the study.
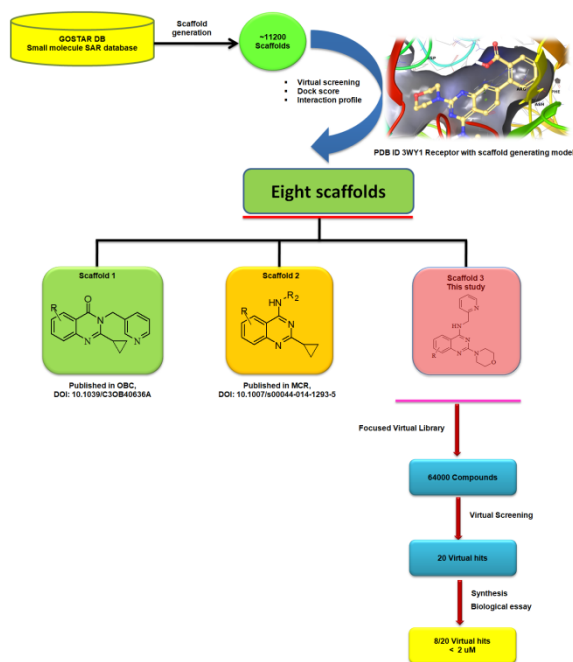
Figure 3. Total workflow of the designing and prioritizing the molecules.

Effect of test compounds on high fat diet/streptozotocin (HFD/STZ) induced hyperglycemic rats: Diabetic rats selected using the above procedure was treated with test compounds and Pioglitazone in between 10-20%. The effect of the test compounds **8**, **13**, **14**, **22** and **27**, on HFD/STZ induced type 2 diabetes mellitus was studied by administering the drugs at a dose of 200 mg/kg BW p.o. and Pioglitazone (2.7 mg/kg p.o.) to the positive control group for 21 days (3 weeks) respect-tively. Fasting blood glucose levels were estimated using glucometer (Accu-chek Active TM Test meter) on day 1, 7, 14 and 21. The percentage reduction in blood glucose levels was estimated and compared with that of normal control and STZ treated (negative control) groups. Data represents mean ±SEM of blood glucose levels in rats treated with test compounds for 21 days. a = represents comparision of blood glucose levels on day 7, 14 and 21 with that of day 1.

2.7. Animals and induction of T2DM

Adult wistar rats of either sex (250-300 g) were procured from the animal house of Bapatla College of Pharmacy (1032/ac/07/CPCSEA), Bapatla, Guntur DT, India and were acclimatized to laboratory conditions one week prior to initiation of experiments in the experimental area, a constant temperature (22±1 °C), relative humidity (40-50%) and 12-12 h light/dark cycles were maintained. The rats were provided with standard chow (Rayan's Biotech, Hyderabad) and water ad libitum. The experimental protocol was approved by Institutional Animal Ethics Committee of Bapatla College of Pharmacy, vide approval no. IAEC/X/4/BCOP/2016. The handling and care of animals was performed in accordance with CPCSEA guidelines for the use and care of experimental animals [36].

2.8. Acute toxicity studies

Acute toxicity studies were performed according to Organization for Economic Co-operation and Development (OECD) guideline 423.Test compounds were administered to six female albino mice fasted for 5hrs at a dose of 2000 mg/kg body weight (limit test) orally. The test was performed in two steps with three animals per step. After each step, mice were observed periodically for 24 hrs and daily for 14 days for signs of toxicity,

3. Results and discussion

3.1. Molecular modelling and drug designing

A molecular modeling study was conducted to predict the binding site of designed molecules in α-glucosidase active site. The ligands were constructed, geometrically optimized, and docked to the X-ray structure of α-glucosidase with high resolution (PDB code 3WY1) obtained from protein data bank which was used for docking and in-silico analysis. Based on in-silico properties 8 core (Figure 3) moieties prioritized for the synthesis and biochemical studies. We have generated 11,268 unique building blocks from our in-house database, GVKBIO online structure activity relation database (GOSTAR), and primary screening was forwarded using these scaffolds against α-glucosidase active site (pdb id 3WY1). Based on the molecular interaction parameters between protein and molecules, binding profile, and docking experiments, eight quinazoline molecular frames were selected for SAR for the bio-evaluation of α-glucosidase enzyme [4].

Acarbose which is considered as reference molecule while designing in this study showed vital interactions with active site of the α-glucosidase. The interactive residues for α-glucosidase are ASP357, ILE358, ILE396, TRP432, ASH398, SER474, PHE601, ALA602, SER474, PHE476, ASP232, ILE233, ARG572, ALA234, PHE236, ASN237, LEU240, TYR240, TRP329, MET470, ASP469, TRP467, TRP565, ARG552, GLY567, ASP568, ARG624, ASP597, HIS626, ALA628, ASP537, and ILE358.Among those above interactive residues ASP357, ASP232, ASP 237, ASP568, ARG552 and HIS626, have formed hydrogen bond with Acarbose (Figure 4), is showing interactive resides between the α-glucosidase and Molecule **16** also showing similar interactions like acarbose, those are PHE37, GLY399, TYR389, ARG400, VAL339, ASP333, HIS332, ARG404, VAL102, TYR65, HIS105, PHE166, ARG200, GLN170, ASH202, PHE147, ILE146, ASP202, THR203, ASN205, PHE206, THR226, LEU227, GLY228, ALA229, PRO230, PHE297, ASN301,

Table 2. IC$_{50}$ values (µM), dock scores for 7-R(different aromatic substituents)-2-morpholino-*N*-(pyridin-2-ylmethyl)quinazolin-4-amine derivatives against α-glucosidase.

| Compound no	R$_1$	IC$_{50}$ (µM) of α-glucosidase	Docking score
8	Phenyl	1.323	-8.1
9	2-Methyl-phenyl	NA	-6.3
10	4-Fluoro-phenyl	NA	-5.7
11	2-Methoxy-phenyl	NA	-6.3
12	4-Methoxy-phenyl	NA	-5.9
13	4-Bi-phenyl	1.310	-8.1
14	3-Methoxy-phenyl	1.122	-8.2
15	3,4-Dimethoxy-phenyl	NA	-4.6
16	4-Cyanophenyl	1.218	-7.9
17	3-Biphenyl	NA	-5.7
18	6-1*H*-Indole	NA	-5.4
19	5-Methylbenzo(1,3)dioxole	NA	-6.1
20	5-1*H*-Indole	NA	-6.0
21	3-Cyanophenyl	NA	-4.6
22	2-Carboxylicphenyl	2.349	-8.1
23	2-Napthyl	NA	-7.7
24	1-Napthyl	NA	-5.3
25	3-Benzofuran	2.140	-8.1
26	4-Methyl-3-amino-phenyl	2.227	-8.0
27	2,4-Dimethoxy-phenyl	1.299	-8.2
Acarbose	Standard drug	0.586	-7.0
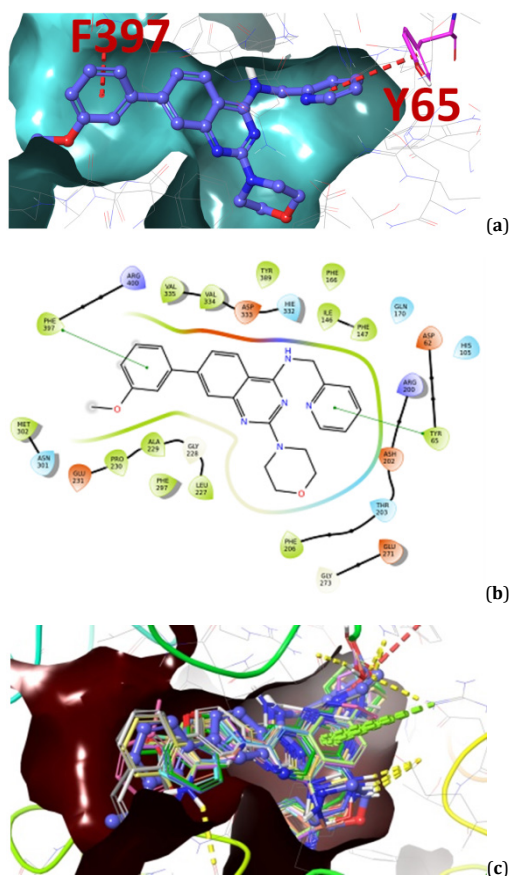
Figure 4. (a) Predicted orientation of the lower energy conformation docked poses of all high score molecules. The binding site was enlarged to show hydrogen bonding (yellow color), centroid of the aromatic ring interactions (green color) between the amino acid residues and best ranked molecules. Amino acid residues that form hydrogen bonds with compound **13**, and it has shown ball and stick blue color carbon skeleton. (b) 2D model: interactive residues with molecule **13**. (c) Overlay of all best scored molecules in the active site of α-glucosidase.

GLU271 and ILE272. Among these, ARG200 has centroid interactions with quinazoline part of the molecule and having within allowed distance (2.5-3.5 Å) further it is also making an important other interaction with TYR235 (centroid interaction). Molecules **16**, **13** and **8** shown good binding affinity towards α-glucosidase active site, but molecule **16** top scored one according to the analysis. Based on their in-silico property analysis we considered for synthesis.

From our previous work the C-4 and C-6 position of the reported quinazoline moiety was well explored for creating SAR of many new chemical entities [23,26], here this work is an extension of the previous report.

We designed, few more novel quinazoline based derivatives by exploring the central moieties at C-7 position The first biochemical screening yielded a considerable activity against α-glucosidase function inhibition i.e. IC$_{50}$ ≤ 1.8 uM, after that we selected a specific molecular frame of quinazoline core

Table 3. *In-vivo* activity of selective molecules.

Treatment	Blood glucose levels (mg/dL) at various intervals (days) [&]			
	1	7	14	21
Control	71.5±4.3 [b#]	68.2±6.1 [b#]	66.1±4.2 [b#]	72.0±6.8 [b#]
Negative control	311.0±6.9	304.6±10.7	307.3±10.5	316.6±9.6
8	316.3±11.8 [bns]	224.4±14.3 [a**b**]	178.4±9.3 [a#b#]	166.1±8.7 [a**b#]
13	281.4±7.3 [bns]	227.2±8.1 [a*b**]	187.6±6.5 [a**b#]	133.5±5.5 [a#b#]
14	301.8±14.1 [bns]	213.1±9.6 [a**b**]	212.8±11.1 [a**b**]	191.0±6.4 [a**b**]
22	317.4±12.7 [bns]	221.3±13.2 [a**b**]	153.5±6.3 [a#b#]	128.5±4.5 [a#b#]
27	298.4±14.3 [bns]	244.6±11.3 [a*b*]	171.7±6.7 [a**b#]	152.3±5.4 [a#b#]
PIO 2.7 mg/kg	304.2±12.1 [bns]	198.3±6.8 [a#b#]	132.4±8.0 [a#b#]	108.4±7.5 [a#b#]

[&] Data represents mean±SEM of blood glucose levels in rats treated with test compounds for 21 days.
[a] Represents comparison of blood glucose levels on day 7, 14 and 21 with that of day 1.
[b] Blood glucose levels of all the groups (n = 6) compared with that of negative control group using one way ANOVA followed by Dunnett's test [30].
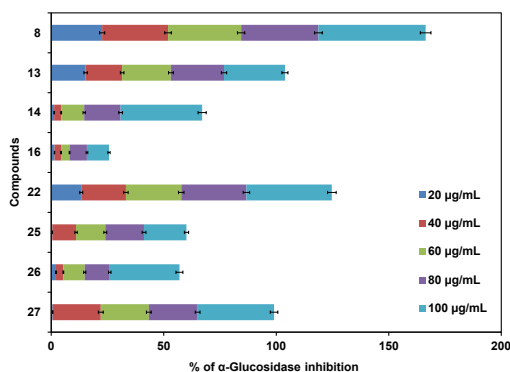

Figure 5. The effect of inhibitor dosage on the response of α-Glucosidase (1 mM) inhibition [27].

moiety and we prepared an SAR which finally resulted in significant activity of the synthesized molecules.

By correctness of holding qualified drug-like properties, each designed chemical entity novel chemical space and based on this through analysis, we prioritized the molecules. The designed novel quinazoline based derivatives which is modified at C-7 position and its final biochemical essay yielded eight molecules with considerable activity (Table 1) i.e. IC_{50} = 1.122, 1.218, 1.299, 1.323, 1.310, 2.140, 2.349 and 2.227 uM, molecule **14**, **16**, **27**, **8**, **13**, **25**, **22** and **26**, respectively. The detailed ADME properties tabulated for all reported molecules in Table 2.

3.2. Biochemical assay of the synthesized compounds (in-vitro study)

In the current study, we have selected the quinazolin-7-chloro scaffold for the generation of a focused library to identify potential inhibitors of α-glucosidase. Compound **8**, with phenyl substitution at 7th position that is 2-morpholino-7-phenyl-*N*-(pyridin-2-ylmethyl) quinazolin-4-amine showed an IC_{50} value of 1.323 μM. The 4-bi-phenyl substituted compound **13** showed IC_{50} value of 1.310 μM and 3-methoxy-phenyl substituted compound, **14**, showed IC_{50} value of 1.122 μM. The IC_{50} values of six compounds **16**, **22**, **25**, **26** and **27** were 1.218, 2.349, 2.140, 2.227 and 1.299 μM, respectively. The reference compound, Acarbose, IC_{50} value is 0.586 μM in the essay. The eight compounds shown similar inhibition compared to reference compound, but unfortunately few other compounds did not show any activity against α-glucosidase (Compounds **9-12**, **15**, **17-21**, **23** and **24**) (Figure 5).

3.3. In-vivo study

Oral glucose tolerance test on 7th and 12th week had shown a protective effect against increase in blood glucose levels in pre-treated groups whereas, no such significant decrease was observed in non-treated groups. In the effect on hypoglycemia, a reduction in blood glucose levels was observed on treatment

with Cycle Inhibiting Factor (CIF) in both pre and post treated rats on 14th and 21st day (Table 3).

3.4. Morphological changes and mortality

Table 3 illustrated the diabetic successful rate (DSR) in rats which were active in *in-vivo* studies where few compounds showed (Compounds **8**, **13**, **14**, **22** and **27**) activity against α-glucodiase inhibition. The *in-silico* and *in-vitro* results are also in accordance with *in-vivo* experimental output. On HFD/STZ induced type 2 diabetes mellitus was studied by administering the drugs at a dose of 200 mg/kg BW p.o. and pioglitazone (2.7 mg/kg p.o.) to the positive control group for 21 days, respectively. Fasting blood glucose levels were estimated using glucometer (Accu-chek Active TM Test meter) on day 1, 7, 14 and 21. The percentage reduction in blood glucose levels was estimated and compared with that of normal control and STZ treated (negative control) groups.

4. Conclusion

Our investigation unveils new C-7 substituted-2-morpholino-*N*-(pyridin-2-ylmethyl)quinazolin-4-amine quinazoline derivatives and significant bioactivity against α-glucosidse inhibition activity. Computational techniques played crucial role while prioritizing the core molecules and as well in structure activity relationship activity of the prioritized molecule **8** of the synthesized molecules out of 20 analogues displayed interesting α-glucosidase activity that is IC_{50} values <2 μM and those lead compounds possesses required physicochemical properties and vital candidates for further lead optimization.

Disclosure statement DS

Conflict of interests: Authors declare no conflict of interest.
Author contributions: All authors contributed equally to this work.
Ethical approval: All ethical guidelines have been adhered.
Sample availability: Samples of the compounds are available from the author.

ORCID iD

Ashok Reddy Ankireddy
http://orcid.org/0000-0001-9621-0907
Gundla Rambabu
http://orcid.org/0000-0003-0390-6505
Tuniki Balaraju
http://orcid.org/0000-0003-2466-1471
Venkanna Banothu
http://orcid.org/0000-0002-4446-8786
Krishna Prasad Gundla
http://orcid.org/0000-0002-2096-1664
Uma Addepally
http://orcid.org/0000-0002-1074-1588
Jithendra Chimakurthy
http://orcid.org/0000-0002-2948-4948

References

[1]. Geiss, L. S.; Wang, J.; Cheng, Y. J.; Thompson, T. J.; Barker, L.; Li, Y.; Albright, A. L.; Gregg, E. W. *Jama* **2014**, *312*, 1218-1226.
[2]. Ferreres, F.; Gil-Izquierdo, A.; Vinholes, J.; Silva, S. T.; Valentao, P.; Andrade, P. B. *Food Chem.* **2012**, *134*, 894-904.
[3]. Bruni, C.; Sica, V.; Auricchio, F.; Covelli, I. *Biochim. Biophys. Acta (BBA)-Enzymol.* **1970**, *212*, 470-477.
[4]. Garlapati, R.; Pottabathini, N.; Gurram, V.; Chaudhary, A. B.; Chunduri, V. R.; Patro, B. *Tetrahedron Lett.* **2012**, *53*, 5162-5166.
[5]. Garlapati, R.; Pottabathini, N.; Gurram, V.; Kasani, K. S.; Gundla, R.; Thulluri, C.; Machiraju, P. K.; Chaudhary, A. B.; Addepally, U.; Dayam, R. *Org. Biomol. Chem.* **2013**, *11*, 4778-4791.
[6]. Chandrika, P. M.; Yakaiah, T.; Rao, A. R. R.; Narsaiah, B.; Reddy, N. C.; Sridhar, V.; Rao, J. V. *Eur. J. Med. Chem.* **2008**, *43*, 846-852.
[7]. Ram, V. J.; Tripathi, B. K.; Srivastava, A. K. *Bioorg. Med. Chem.* **2003**, *11*, 2439-2444.
[8]. Koh, K. K.; Park, S. M.; Quon, M. J. *Circulation* **2008**, *117*, 3238-3249.
[9]. Saltiel, A. R.; Olefsky, J. M. *Diabetes* **1996**, *45*, 1661-1669.
[10]. De Melo, E. B.; Gomes, A. S.; Carvalho, I. *Tetrahedron* **2006**, *62*, 10277-10302.
[11]. Landgraf, R. *Drugs Aging* **2000**, *17*, 411-425.
[12]. Sinclair, A. J. International textbook of Diabetes mellitus, Wiley, Worcestershire, United Kingdom, 2004.
[13]. Wan, Z. K.; Wacharasindhu, S.; Levins, C. G.; Lin, M.; Tabei, K.; Mansour, T. S. *J. Org. Chem.* **2007**, *72*, 10194-10210.
[14]. Goto, S.; Tsuboi, H.; Kanoda, M.; Mukai, K.; Kagara, K. *Org. Proc. Res. Dev.* **2003**, *7*, 700-706.
[15]. Friesner, R. A.; Murphy, R. B.; Repasky, M. P.; Frye, L. L.; Greenwood, J. R.; Halgren, T. A.; Sanschagrin, P. C.; Mainz, D. T. *J. Med. Chem.* **2006**, *49*, 6177-6196.
[16]. Rosenstock, J.; Brazg, R.; Andryuk, P. J.; Lu, K.; Stein, P.; Study, S. *Clin. Therap.* **2006**, *28*, 1556-1568.
[17]. Yamaguchi, T.; Sakairi, K.; Yamaguchi, E.; Tada, N.; Itoh, A. *RSC Adv.* **2016**, *6*, 56892-56895.
[18]. Ghavami, A.; Johnston, B. D.; Pinto, B. M. *J. Org. Chem.* **2001**, *66*, 2312-2317.
[19]. Andrews, J. S.; Weimar, T.; Frandsen, T. P.; Svensson, B.; Pinto, B. M. *J. Am. Chem. Soc.* **1995**, *117*, 10799-10804.
[20]. Flanagan, P. R.; Forstner, G. G. *Biochem. J.* **1978**, *173*, 553-563.
[21]. Balaraju, T.; Kumar, A.; Bal, C.; Chattopadhyay, D.; Jena, N.; Bal, N. C.; Sharon, A. *Struc. Chem.* **2013**, *24*, 1499-1512.
[22]. Khan, I.; Ibrar, A.; Abbas, N.; Saeed, A. *Eur. J. Med. Chem.* **2014**, *76*, 193-244.
[23]. Gurram, V.; Garlapati, R.; Thulluri, C.; Madala, N.; Kasani, K. S.; Machiraju, P. K.; Doddapalla, R.; Addepally, U.; Gundla, R.; Patro, B. *Med. Chem. Res.* **2015**, *24*, 2227-2237.
[24]. Iino, T.; Sasaki, Y.; Bamba, M.; Mitsuya, M.; Ohno, A.; Kamata, K.; Hosaka, H.; Maruki, H.; Futamura, M.; Yoshimoto, R. *Bioorg. Med. Chem. Lett.* **2009**, *19*, 5531-5538.
[25]. Thiyagarajan, A.; Salim, M. T.; Balaraju, T.; Bal, C.; Baba, M.; Sharon, A. *Bioorg. Med. Chem. Lett.* **2012**, *22*, 7742-7747.
[26]. Gurram, V.; Akula, H. K.; Garlapati, R.; Pottabathini, N.; Lakshman, M. K. *Adv. Syn. Catal.* **2015**, *357*, 451-462.
[27]. Liu, J. F.; Lee, J.; Dalton, A. M.; Bi, G.; Yu, L.; Baldino, C. M.; McElory, E.; Brown, M. *Tetrahedron Lett.* **2005**, *46*, 1241-1244.
[28]. Hikawa, H.; Ino, Y.; Suzuki, H.; Yokoyama, Y. *J. Org. Chem.* **2012**, *77*, 7046-7051.
[29]. Garlapati, R.; Pottabathini, N.; Gurram, V.; Kasani, K. S.; Gundla, R.; Thulluri, C.; Machiraju, P. K.; Chaudhary, A. B.; Addepally, U.; Dayam, R.; Chunduri, V. R.; Patro, B. *Org. Biomol. Chem.* **2013**, *11*, 4778-4791.
[30]. Kasula, M.; Balaraju, T.; Toyama, M.; Thiyagarajan, A.; Bal, C.; Baba, M.; Sharon, A. *Chem. Med. Chem.* **2013**, *8*, 1673-1680.
[31]. Balaraju, T.; Kumar, A.; Bal, C.; Chattopadhyay, D.; Jena, N.; Bal, N. C.; Sharon, A. *Struc. Chem.* **2013**, *24(5)*, 1499-1512.
[32]. Bal, N. C.; Jena, N.; Sopariwala, D.; Balaraju, T.; Shaikh, S.; Bal, C.; Sharon, A.; Gyorke, S.; Periasamy, M. *Biochem. J.* **2011**, *435(2)*, 391-399.
[33]. Thiyagarajan, A.; Salim, M. T. A.; Balaraju, T.; Bal, C.; Baba, M.; Sharon, A. *Bioorg. Med. Chem. Lett.* **2012**, *22(24)*, 7742-7747.
[34]. Kumar, A.; Chakravarty, H.; Bal, N. C.; Balaraju, T.; Jena, N.; Misra, G.; Bal, C.; Balaraju, T.; Jena, N.; Misra, G.; Pieroni, E.; Periasamy, M.; Sharon, A. *Mol. Biosys.* **2013**, *9(7)*, 1949-1957.
[35]. Bal, N. C.; Jena, N.; Chakravarty, H.; Kumar, A.; Chi, M.; Balaraju, T.; Rawale, S. V.; Sharon, A.; Periasamy, M. *Biopolymers* **2015**, *103(1)*, 15-22.
[36]. Talasila, M.; Bavirisetti, H.; Chimakurthy, J.; Candasamy, M. *J. Health Sci.* **2014**, *4(3)*, 162-168.